IEEE Access
Multidisciplinary | Rapid Review | Open Access Journal

Received November 6, 2018, accepted November 27, 2018, date of publication December 4, 2018,
date of current version January 11, 2019.

Digital Object Identifier 10.1109/ACCESS.2018.2885019

A Novel Control Scheme for Aircraft Engine Based on Sliding Mode Control With Acceleration/Deceleration Limiter

BING YU, HONGWEI KE, WENJUN SHU, AND TIANHONG ZHANG
Jiangsu Province Key Laboratory of Aerospace Power System, Nanjing University of Aeronautics and Astronautics, Nanjing 210016, China
Corresponding author: Bing Yu (yb203@nuaa.edu.cn)

This work was supported by the Fundamental Research Funds for the Central Universities under Grant NS2018017.

ABSTRACT To provide the desired thrust and prevent the engine from exceeding any safety or operational limits, a min–max selector with linear limiters is widely employed in current aircraft engine control logic. However, with the further requirements of engine performance, the traditional linear limiters should be improved. Though there are many researchers working on the development of improvement methods, none of those methods consider the limitation of core shaft acceleration. In this paper, a novel control scheme for aircraft engine based on sliding mode control with acceleration/deceleration limiter is proposed. Above all, the controller construction process is introduced, and the asymptotic stability of the whole controller is given. Then, with linearized model of JT9D turbofan engine, the control performance of the new approach is presented, which is also compared with the traditional methods. The simulation results show that the proposed method is efficient, and it can ensure all outputs of the controller, including the core shaft acceleration $\dot{N}_c$, high-pressure turbine outlet temperature increment ΔT_{48}, high-pressure compressor stall margin increment $\Delta SmHPC$, and so on, are well controlled.

INDEX TERMS Min-max logic, sliding mode control, aircraft propulsion, acceleration/deceleration limit.

I. INTRODUCTION

During the tracking process of the aircraft engine control, it must be ensured that all the constrained outputs (such as temperature, surge margin, speed, and pressure, etc.) be within the allowable working range. Otherwise, it will affect the life of an engine or even lead to the appearance of engines' undesirable characteristics, which will cause the failure of the engine and bring a series of serious consequences [1]–[4]. Therefore, how to play a good performance of the aircraft engine under the limit protection becomes a key problem in its control research [5]. In a word, the engine controller has to satisfy two types of requirements: performance and safety [6].

To guarantee the desired thrust and prevent the engine from exceeding any operational limit, the Min-Max structure is widely utilized in engines' control. The Min-Max logic, which is also known as ''override logic'' or ''selector control'', includes many measured signals but one actuator, and is applied to control output constrained systems successfully [7]. The structure was firstly adopted in 1970s, and had been proven an efficiency approach in aircraft engine control [7], [8].

Traditional aircraft engine control system employs linear regulators adopting the Min-Max structure to achieve the constraint management [6], [9], [10]. In recent years, research results show that the traditional Min-Max linear control structure has certain conservatism in the constraint treatment, which may decline the speed of engines' dynamic response [11], [12]. To overcome this problem, several typical research works have been carried out and which are all proven to be effective. May and Garg [13] reported the concept of using Conditionally Active (CA) limit regulators in the Min-Max architecture of typical engine control laws. The CA architecture in the Min-Max scheme only activates the limit regulators when the operating point is within a certain bound of the limit and approaching the limit at a faster rate than the prescribed one. Yuan and Zhao [14] used the active disturbance rejection control (ADRC) to design the limit protection controller, which can carry the point of limit protection while making the control system responses quickly. Imani and Montazeri-Gh [15] presented a strategy to design linear regulators of Min-Max selector control to improve transient limit protection by using

Linear Matrix Inequalities (LMI) approach. Ilya *et al*. [16] proposed a limit protection method based on robust control and robust reference regulator, focused on the study and control of the inlet distortion caused by uncertainty, and achieved better control results than the linear regulator. Research conducted by Ritcher *et al*. [17]–[19] indicated that many shortcomings of the standard Min–Max approach can be removed by replacing linear regulators with Sliding Mode Control (SMC) regulators, and the dynamic performance of the engine is also improved. It can be considered as an effective approach to improve Min-Max limit protection in aircraft engine control, and researchers have expressed a strong research interest in it. Articles about this aspect are also frequently reported recently. For example, in 2018, Imani and Montazeri-Gh [20] presented a multi-input, multi-output scheme based on sliding-mode control, and a new switching logic is proposed for set point tracking in aero engines subject to output constraints. In controller design process, they use state feedback techniques and convex optimization problem to determine the limit values of the variables which are affected by engine acceleration or deceleration. And the simulation results show the efficient performance of this method. In the same year, Tenghui *et al*. [20] designed a sliding mode controller based on fuzzy-PID approaching law for aero engine with strong nonlinearity. And the simulation results showed the new controller is better in suppressing chattering than other controller and the impact of quickness is not large, which prove the validity of this controller.

However, none of those improvement methods consider the limitation of core shaft acceleration. It is well known that the core shaft acceleration without limit will cause the engine working under some extremely harsh conditions. So that many important parts of the engine will damage sooner, it will lead to the decrease in engine life and reduce the economics of the engine. So with the purpose to extend the working life of the engine, researchers proposed to introduce acceleration limits on the aircraft engine control, and results show that the blade life can be increased by nearly 30% compared with the original when the speed rise time is constant [22], [23].

In this paper, the limitation of core shaft acceleration is put into the aircraft engine control during the tracking process. The specific idea is: in addition to limit placed on the magnitudes of critical variables such as turbine temperature, shaft speeds, combustor pressure, and engine pressure ratio, the core shaft acceleration must also be maintained between prescribed bounds. An upper bound is introduced to protect the engine against surge and stall, while a lower limit is introduced to provide safety against engine flame-out.

In view of the sliding mode control method has been successfully carried out in aircraft engine control [19], [24], aircraft control [25], [26], auto cruise [27], and other fields successfully launched a simulation analysis and application. This paper proposed a novel control scheme for aircraft engine based on sliding mode control with acceleration/deceleration limiter and the method is named with

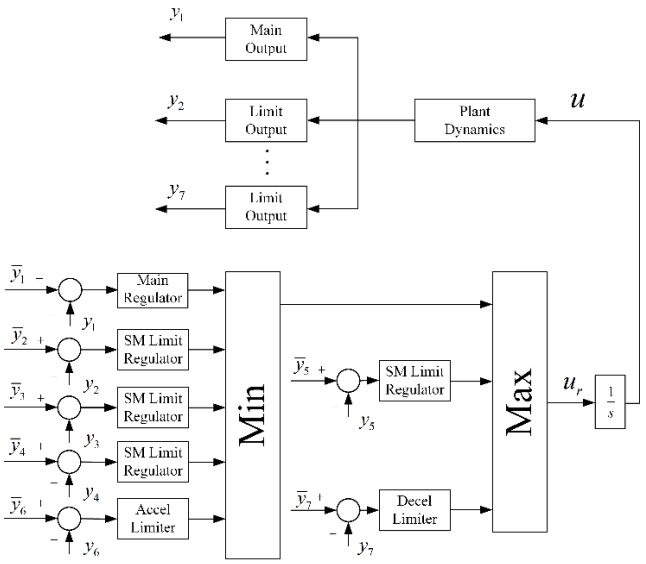

FIGURE 1. The control logic of Min-Max/SMC.

Min-Max/SMC control logic. Section II, the Min-Max/SMC control logic and its proof of stability are introduced. Section III is the design process of the acceleration/deceleration limiter with new method. In section IV, different acceleration/deceleration limiters are applied to the linearized model of a typical two-spool turbofan engine JT9D and some analysis are made. Section V is the conclusion.

II. MIN-MAX/SMC CONTROL METHOD

Min-Max/SMC method is a limit protection of sliding mode control method which adopts Min-Max structure. The main idea of which is to define different sliding variables for each limit output and the main control output. The sliding variable corresponding to the limit output variable is designed by the method which is similar to the main regulator, and it is defined as the difference between the output and the limit value. Currently, since the thrust of the engine cannot be directly measured by sensors, it is necessary to use a substitute variable that can be reliably measured to express the thrust. In practice, fan speed (N_f) or engine pressure ratio (EPR) feedback loop is often used to control the thrust indirectly. In this paper, N_f is chosen as the main control output variable. In order to meet the requirement that the main output is precisely regulated, integration is used at the input section of the engine model. And the control logic is shown in Fig. 1. Generally, when the main regulator is active, it means that its output u_r is minimum in the Min selector while is maximum in the Max selector. But when one or more limit outputs have the trend to exceed the limit or even have already exceeded the limit, corresponding limit regulators will be active and replace the main regulator for output. For example, when high pressure turbine outlet temperature increment (ΔT_{48}) is going to exceed or have exceeded its limit, its limit regulator will be active that $u_r = u_{r\Delta T_{48}}$.

The switching law of Min-Max structure in the Fig. 1 can be expressed as:

$$q = \max_{j\in H}\left\{\min_{j\in L}\{u_{ri}\}, u_{rj}\right\} \tag{1}$$

As shown in Fig. 1, $L = \{1, 2, 3, 4, 6\}$, and it is the regulator index connected by the low selection operation. And $H = \{5, 7\}$, which is the regulator index connected by the high selection operation.

A. MAIN REGULATOR DESIGN

Similar to the proof process in Richter's article [19], with the purpose of introducing the design of sliding mode method in the main regulator briefly, a steady state point model of the engine is used as an example to illustrate, and the following is the expression in state space.

$$\dot{\boldsymbol{x}} = \boldsymbol{A}\boldsymbol{x} + \boldsymbol{B}u \tag{2}$$

$$\dot{u} = u_r \tag{3}$$

$$y = \boldsymbol{C}\boldsymbol{x} \tag{4}$$

Where, $\boldsymbol{x} = [x_1\ x_2]^T = [\Delta N_f\ \Delta N_c]^T$, which is composed of fan speed increment and core speed increment. The control input u is fuel flow rate, u_r is the fuel flow increment (ΔW_f), and y is the system output, which is fan speed increment.

Here, $\boldsymbol{A}$ is a $n \times n$ non-singular matrix and $(\boldsymbol{A}, \boldsymbol{B})$ is controllable. Auxiliary output is defined for this system.

$$y = \boldsymbol{E}\boldsymbol{x} + Fu \tag{5}$$

Where, $\boldsymbol{E}$ and F are sliding mode coefficients to be designed, and $\boldsymbol{E}$ is a vector while F is a scalar.

Then, the sliding function can be defined as:

$$s = y - \bar{y} \tag{6}$$

Where, $\bar{y}$ is a constant that achieves $y = r$ at steady state. Eq. (6) is used to find the derivative of s. Cause $\bar{y}$ is a constant, so its derivative equals to 0, and the derivative of s can be rewritten as:

$$\dot{s} = \dot{\boldsymbol{y}} = \boldsymbol{E}\dot{\boldsymbol{x}} + F\dot{u} \tag{7}$$

And in this paper, Lyapunov function can be written as:

$$L = \frac{1}{2}s^2 \tag{8}$$

The exponential approach law [28], which is used in this paper can be expressed as:

$$\dot{s} = -\eta * \mathrm{sgn}(s) \tag{9}$$

Where, η is a positive number, and sgn() is the sign function.

So the derivative form of Lyapunov function can be written as:

$$\dot{L} = \dot{s}s = -\eta * \mathrm{sgn}(s) * s \le 0 \tag{10}$$

With the establishment of this inequality, the asymptotic stability of the main control loop can be guaranteed. Then according to (7) and (9), the following equation can be gotten.

$$\dot{s} = \boldsymbol{E}\begin{bmatrix}\boldsymbol{A} & \boldsymbol{B}\end{bmatrix}\boldsymbol{x}_a + Fu_r = -\eta * \mathrm{sgn}(s) \tag{11}$$

Where, $\boldsymbol{x}_a = \begin{bmatrix}\boldsymbol{x}^T & u\end{bmatrix}^T$ is defined as the augmented state.

Then, the sliding mode control law expression can be gotten:

$$u_r = -\frac{1}{F}(\boldsymbol{E}\begin{bmatrix}\boldsymbol{A} & \boldsymbol{B}\end{bmatrix}\boldsymbol{x}_a + \eta * \mathrm{sgn}(s)) \tag{12}$$

From the definition of s, when it equals to zero, the equation $y = \bar{y}$ must be satisfied. And in order to associate the control rate with state of the object, substituting $u = \frac{1}{\Theta}(\boldsymbol{E}\boldsymbol{x} - \bar{y})$ into the state space (2) yields the following expression:

$$\dot{x} = \left(\boldsymbol{A} - \frac{\boldsymbol{B}\boldsymbol{E}}{F}\right)\boldsymbol{x} + \frac{\boldsymbol{B}}{F}\bar{y} = \boldsymbol{A}_{eq}\boldsymbol{x} + \frac{\boldsymbol{B}}{F}\bar{y} \tag{13}$$

Where, $\boldsymbol{A}_{eq}$ equals to $\left(\boldsymbol{A} - \frac{\boldsymbol{B}\boldsymbol{E}}{F}\right)$.

If $F \neq 0$ and $\boldsymbol{A}_{eq}$ satisfies that all the eigenvalues of itself has negative real part, then a steady state can be reached. Under this circumstance, $\dot{\boldsymbol{x}} = \boldsymbol{0}$, $\boldsymbol{x} = \bar{\boldsymbol{x}}$ is the steady state. And the poles of $\boldsymbol{A}_{eq}$ can be configured by choosing suitable $\boldsymbol{E}$ and F, so that the desirable time constant and damping values can be gotten.

$$\bar{\boldsymbol{x}} = -(\boldsymbol{A}_{eq})^{-1}\frac{\boldsymbol{B}}{F}\bar{\boldsymbol{y}} \tag{14}$$

The steady state value of output variable is $\boldsymbol{C}\bar{x}$, and let it equal to r, then the required $\bar{y}$ can be expressed as:

$$\bar{y} = -\frac{Fr}{\boldsymbol{C}\boldsymbol{A}_{eq}^{-1}\boldsymbol{B}} \tag{15}$$

B. LIMIT PROTECTION CONTROLLER DESIGN

For engine output variables such as high pressure turbine outlet temperature (T_{48}), high pressure compressor outlet static pressure (P_{s30}) and etc., the equations can be defined as:

$$y_i = \boldsymbol{C}_i\boldsymbol{x} + D_i u, \quad (D_i \neq 0) \tag{16}$$

For such output variables, if the eigenvalues of $\boldsymbol{A}_{eq,i}$ have negative real part, it is not necessary to design the sliding mode coefficients. The coefficients obtained by linearization are equal to the sliding coefficients, $\boldsymbol{E}_i = \boldsymbol{C}_i, F_i = D_i$. Defining the sliding function as $s_i = y_i - \bar{y}_i$, and the control law can be obtained with (7) to (12).

$$u_{ri} = -\frac{1}{F_i}(\boldsymbol{E}_i\begin{bmatrix}\boldsymbol{A} & \boldsymbol{B}\end{bmatrix}\boldsymbol{x}_a + \eta_i * \mathrm{sgn}(s_i)) \tag{17}$$

The control law (17) can ensure $y_i \le \bar{y}_i$, so that the output variable does not exceed its limit value.

TABLE 1. The rules of the logical type.

Limit type	Symbol of K_i	Selector
upper	+	Min
upper	-	Max
lower	+	Max
lower	-	Min

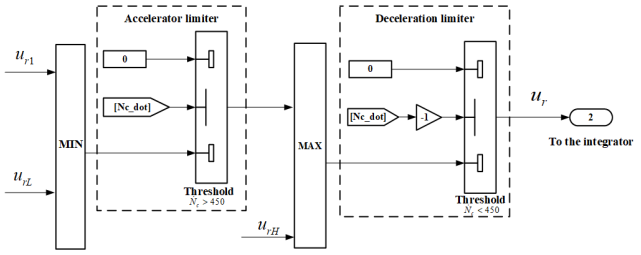

FIGURE 2. Schematic of JT9D Min–Max arrangement with acceleration and deceleration limiters.

C. CONTROLLER CHARACTERISTICS AND STABILITY

Min-Max/SMC method has been proved to be asymptotically stable under certain conditions, and it can be ensure that the steady-state error converges to zero. Since the proof process is very complex, the stability conditions are summarized in the following two lemmas. As for the derivation details of the system, readers can refer to [17] and [18]. Also, the maximum and minimum selector type, the upper and the lower limit of the variable requirements, and the relationships of K_i are shown in Table 1 [17].

Defining the augmented state as $\boldsymbol{x}_a = \begin{bmatrix} \boldsymbol{x}^T & u \end{bmatrix}^T$, and $\overline{\boldsymbol{x}}_{ai} = \begin{bmatrix} \overline{\boldsymbol{x}}_i^T & \overline{u}_i \end{bmatrix}^T$, where $i \in L \cup H$.

1) LEMMAS 1

In the Min-Max switching law (1), $\begin{bmatrix} \overline{\boldsymbol{x}}_{i^*}^T & \overline{\boldsymbol{u}}_{i^*} \end{bmatrix}^T$ represents the system parameters of unique equilibrium point, where $i^* \in L \cup H$ is an index which satisfies the following (18) and (19) or satisfies the (19) and (20):

$$0 \leq -\frac{\operatorname{sgn}\left(\Delta_{j,i^*}\right)}{D_j}, \quad (j \in L) \tag{18}$$

$$0 \geq -\frac{\operatorname{sgn}\left(\Delta_{j,i^*}\right)}{D_j}, \quad (j \in H) \tag{19}$$

$$0 > \min_{j \in L} \left\{ -\frac{\operatorname{sgn}\left(\Delta_{j,i^*}\right)}{D_j} \right\} \tag{20}$$

Where, $\boldsymbol{J}_j = \begin{bmatrix} \boldsymbol{C}_j & D_j \end{bmatrix}$, $\Delta_{j,i} = \boldsymbol{J}_j \left(\overline{\boldsymbol{x}}_{ai} - \overline{\boldsymbol{x}}_{aj}\right)$, and $\Delta_{j,i}$ is the value in channel j when channel i is active.

2) LEMMAS 2

Under the control input (17) and Min-Max switching law, all trajectories of system, (2) and (3) converge asymptotically to the unique equilibrium point $\overline{\boldsymbol{x}}_{i^*}$.

D. ACCELERATION/DECELERATION LIMITER DESIGN

In order to solve the design issues of the $\dot{\boldsymbol{N}}_c$ limiter in the case that $\dot{\boldsymbol{N}}_c$ cannot be measured directly, in this paper, the core speed is used as the limited output. The acceleration upper limiter design process is shown with follows.

According to (2), the core speed can be expressed as $N_c = \boldsymbol{C}_2\boldsymbol{x} = \begin{bmatrix} 0 & 1 \end{bmatrix}\boldsymbol{x} = x_2$.

Its auxiliary output is:

$$y_6 = \boldsymbol{E}_6\boldsymbol{x} + F_6 u \tag{21}$$

And (7) can be expressed as:

$$\overline{y_6} = -\frac{F_6 r_6}{\boldsymbol{C}_2 \boldsymbol{A}_{eq,6}{}^{-1} \boldsymbol{B}} \tag{22}$$

Where, $\boldsymbol{A}_{eq,6}$ equals $\left(\boldsymbol{A} - \frac{\boldsymbol{B}\boldsymbol{E}_6}{F_6}\right)$, and r_6 is the limit value of core speed. Also, $\boldsymbol{E}_6$ and F_6 are given. $\overline{y_6}$ is a constant.

The sliding function is defined as $s_6 = y_6 - \overline{y}_6$, and the sliding mode control law can be described as follows:

$$u_{r6} = -\frac{1}{F_6}(\boldsymbol{E}_6 \begin{bmatrix} \boldsymbol{A} & \boldsymbol{B} \end{bmatrix} \boldsymbol{x}_a + \eta_6 * \operatorname{sgn}(s_6)) \tag{23}$$

Let $\boldsymbol{A}$ equals to $\begin{bmatrix} a_{11} & a_{12} \\ a_{21} & a_{22} \end{bmatrix} = \begin{bmatrix} \boldsymbol{A}_1 \\ \boldsymbol{A}_2 \end{bmatrix}$, and $\boldsymbol{B}$ equals to $\begin{bmatrix} b_1 \\ b_2 \end{bmatrix}$. Then they are substituted into Eq. (2), so the core speed can be expressed as:

$$\dot{x}_2 = \boldsymbol{A}_2\boldsymbol{x} + b_2 u \tag{24}$$

Let $\boldsymbol{E}_6$ equals to $\boldsymbol{A}_2$, and F_6 equals to $b_2 + \delta_{b_2}$ which is approximately equal to b_2. So all the eigenvalues of $\boldsymbol{A}_{eq,6}$ can have negative real parts, then the following equation can be gotten.

$$\dot{x}_2 \approx y_6 \tag{25}$$

The above equation makes the auxiliary output defined for core speed N_c equal to core acceleration, and the sliding mode control law, whose specific form of expression is Eq. (23), makes $y_6 \leq \overline{y_6}$, that is $\dot{N}_c = \dot{x}_2 \leq \overline{y_6}$. Let $\overline{y_6}$ equals to $\overline{\dot{N}_c}$, and the limit r_6 can be calculated through Eq. (22), where $\overline{\dot{N}_c}$ is a constant greater than zero.

As shown in the Fig. 1, the core shaft acceleration limiter is set to be selected by the Min selector, which is determined by the specific data. $\overline{\dot{N}_c}$ is a positive number, whose upper limit is restricted. And b_2 is usually a positive number, so the min selector is used to select its value. In addition, the stability condition should be satisfied for the core acceleration limiter is Lemma 1. Similarly, when it comes to the designing process of the deceleration limiter, Lemma 1 should be satisfied, too. With the fact that it is set to be a max selector, and $\overline{\dot{N}_c}$ is a negative number, b_2 should be a positive number. These results can guide the definition of the parameters using in the controller.

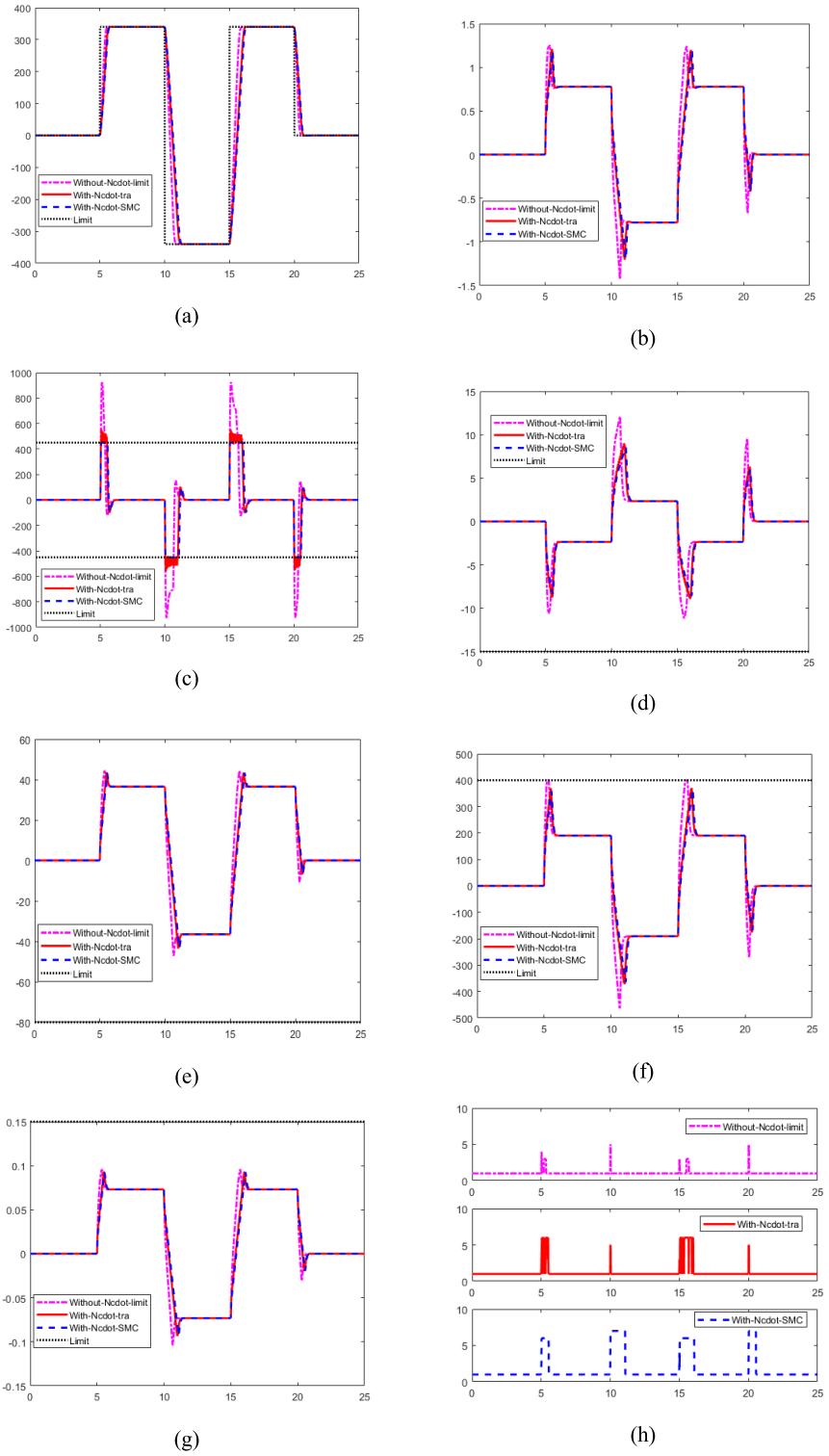

FIGURE 3. The results of simulation. Graph (a) indicates the response of fan speed. Graph (b) indicates the input of fuel flow. Graph (c) indicates the output N_c. Graph (d) indicates lower limited output $\Delta SmHPC$. Graph (e) indicates lower limited output ΔP_{s30}. Graph (f) indicates upper limited output ΔT_{48}. Graph (g) indicates upper limited output ΔEPR. Graph (h) indicates the switching history. In these graphs, the dash dot line (in fuchsia) refers to the situation without $\dot{N}_c$ limit, the line (in red) refers to the situation that limits $\dot{N}_c$ with the traditional way, the dotted line (in blue) refers to the situation that limits $\dot{N}_c$ with SMC limiter, and the dotted line (in black) refers to the limit line.

III. RESULTS AND DISCUSSION

A. MODEL INTRODUCTION AND CONTROL PARAMETER DESIGN

To show the effectiveness of the acceleration/deceleration limiter design method, a two-spool turbofan engine linearized model is used to verify the designed controller's performance. And it is obtained from the open source engine model JT9D which is provided by the NASA Glenn research center. The inlet condition is at total temperature of 833.72 K and total pressure of 38.11 kPa. There are four constrained outputs. Each of the following values is obtained by the linearization tool.

$$\begin{cases} \mathbf{A} = \begin{bmatrix} -4.1928 & 2.9202 \\ 1.7508 & -6.6758 \end{bmatrix} & \mathbf{B} = \begin{bmatrix} 929.34 \\ 1297.6 \end{bmatrix} \\ \boldsymbol{E_2} = \begin{bmatrix} 0.056458 & -0.066678 \end{bmatrix} & F_2 = -7.074 \\ \boldsymbol{E_3} = \begin{bmatrix} -1.1969 & 1.6622 \end{bmatrix} & F_3 = 254.09 \\ \boldsymbol{E_4} = \begin{bmatrix} -0.0037 & 0.1599 \end{bmatrix} \times 10^{-3} & F_4 = 0.0461 \\ \boldsymbol{E_5} = \begin{bmatrix} 0.021912 & 0.059543 \end{bmatrix} & F_5 = 18.92 \end{cases} \tag{26}$$

Where, the indexes 2, 3, 4, and 5 are respectively high pressure compressor stall margin ($SmHPC$), T_{48}, EPR, and compressor outlet pressure (P_{s30}). It can be verified that these outputs all satisfy that the eigenvalues of their characteristic equations contain negative real parts, which can guarantee the stability of the controller.

Through the analysis above, a conclusion can be drawn that this system model is open-loop stable. The main regulator is aimed at the fan speed, that is $y_1 = \begin{bmatrix} 1 & 0 \end{bmatrix} \boldsymbol{x} = x_1$. The pole placement method used to solve this problem is to configure $\boldsymbol{A}_{eq,1}$ to have its eigenvalues at -3.24 and -10.25, and take $F_1 = 1$, then

$$\boldsymbol{E_1} = [-0.0008 \quad 0.0026] \tag{27}$$

The sliding coefficients of acceleration and deceleration regulators are:

$$\begin{aligned} \boldsymbol{E_6} = \boldsymbol{E_7} &= \begin{bmatrix} 0.5080 & -2.1737 \end{bmatrix} \\ F_6 = F_7 &= 891.1433 \end{aligned} \tag{28}$$

Each limit value used in this paper is the common commercial engine limits as shown in the Table 2 [17], and it should be noted that y_6 and y_7 can be different in practice.

A simple calculation can be used to ensure that the eigenvalues of $\boldsymbol{A}_{eq,6}$ and $\boldsymbol{A}_{eq,7}$ are negative and meet the condition. And all the limiters meet Lemma 1, especially $\Delta_{6,1} = -450$ and $\Delta_{7,1} = 450$.

In order to reduce chattering, the sign function in sliding mode control law is replaced by a saturation function [28], that is:

$$\text{sat}(s) = \begin{cases} sgn(s), & s \geq \emptyset \\ \dfrac{s}{\emptyset} \end{cases} \tag{29}$$

TABLE 2. The output limit.

Variables	Limits
ΔSmHPC	$y_2 \geq \overline{y_2} = -15\%$
ΔT_{48}	$y_3 \leq \overline{y_3} = 400^{\circ}R$
ΔEPR	$y_4 \leq \overline{y_4} = 0.15$
ΔP_{s30}	$y_5 \geq \overline{y_5} = -80psi$
$\dot{N}_c$	$y_6 \leq \overline{y_6} = 450rpm/s$ or $y_7 \geq \overline{y_7} = -450$rpm/s

The values of η_i and the boundary layer ϕ_i in the saturation can be obtained through simple debugged. And the final value is as follows:

$$\eta_1 = 20F_1, \quad \eta_i = 15F_i (i = 2 \ldots 7) \tag{30}$$

$$\phi_1 = 1, \quad \phi_2 = 0.1, \ \phi_3 = 0.01$$
$$\phi_4 = \phi_5 = 1, \quad \phi_6 = \phi_7 = 0.005 \tag{31}$$

B. SIMULATION RESULTS

In order to evaluate the performance of the newly proposed method, a conventional way of maintaining the acceleration between specified boundaries in a commercial engine, referred to as an override switch, is introduced here as a reference. The specific idea is to override the value of u_r, which is calculated by the min-selected regulators, with a constant rate of zero pps/s whenever the acceleration reaches its upper limit [18]. And the acceleration is maintained by replacing the rate produced by the max stage with $u_r = 0$ whenever the acceleration reaches its lower limit. The specific architecture of this method is shown in the Fig. 2. In this paper, this method is used as the reference for the performance evaluation of the acceleration/deceleration limiter designed by the new proposed method.

Fig. 3a shows the system response in tracking the desired fan speed. The settling time is about the same in both of methods, and longer than the response without the $\dot{N}_c$ limiter. Incremental fuel flow input has been shown in Fig. 3b. Fig. 3c shows that without the $\dot{N}_c$ limiter, the output $\dot{N}_c$ will just exceed the limit, and it may be too big. The tradition $\dot{N}_c$ limiter will frequently switch the switch, and $\dot{N}_c$ exceeds the limit too. But the proposed $\dot{N}_c$ limiter can keep $\dot{N}_c$ within ± 450 without chattering. This can prove that the new method is effective and has a better performance. Specifically, the transition is smoother and the process is not overrun.

Fig. 3d, Fig. 3e, Fig. 3f, and Fig. 3g are the outputs of $\Delta SmHPC$, ΔT_{48}, ΔP_{s30}, and ΔEPR. It can be seen from the figures that all controllers satisfy constrains. Due to the limit of $\dot{N}_c$, these outputs are forced to be more conservative, and it should be noticed that the performances of the two methods are almost the same. Fig. 3h shows the switching history. It demonstrates that 1) after a while response time the active channel is $i = 1$ which means the main regulator is active. 2) In the acceleration phase about 5 seconds and 15 seconds acceleration limiter is active and deceleration phase about

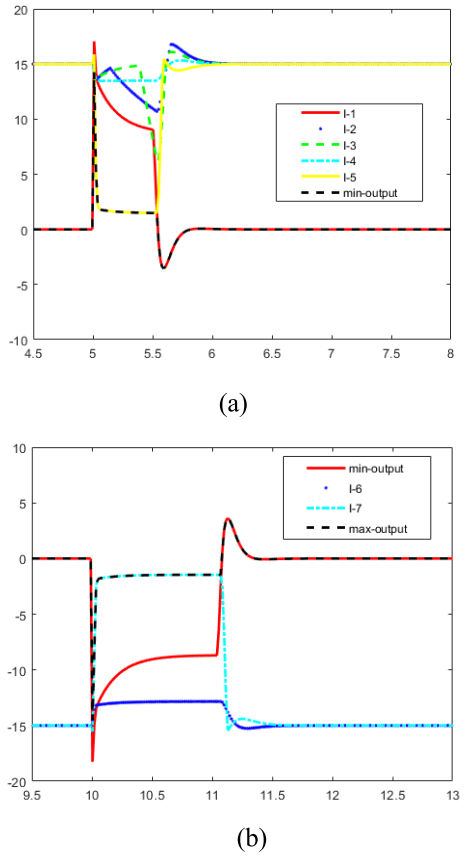

FIGURE 4. The fuel flow rate of different selectors. Graph (a) indicates the min selector fuel flow rate in the acceleration. Graph (b) indicates the max selector fuel flow rate in the deceleration. The dotted line (in black) refers to the real output of the selectors, while the other lines named with $I-i, (i=1,2,3,4,5,6,7)$ refer to the output of the different limiters.

10 seconds and 20 seconds deceleration limiter is active, the two limiters did not interfere with each other. And with the comparison of the results of the three situations, a conclusion can be drawn that with the new method, the number of switching is greatly reduced, which can greatly improve the effectiveness of the system and reduce the possibility of controller error.

Fig.4a and Fig. 4b show the min selector fuel flow rate in the acceleration and the max selector fuel flow rate in the deceleration, respectively. The specific selection process of the fuel flow rate can be seen intuitively.

In this paper, the thrust is indirectly controlled through fan speed feedback loop N_f. If the acceleration limiting is applied to N_f, reference ramps are usually commanded for this variable [18]. But in principle, a similar acceleration limiter proposed by this paper can be applied to $\dot{N}_f$. In this paper, N_f is limited to less than 250rpm/s. Fig. 5a shows the fan speed response for reference ramp and $\dot{N}_f$ limiters. It can be seen that with $\dot{N}_f$ limiters, the response is faster than the situation with reference ramp input. Fig. 5b shows that though $\dot{N}_f$ has a quicker response under the traditional method, the numerical value of $\dot{N}_f$ changes drastic which

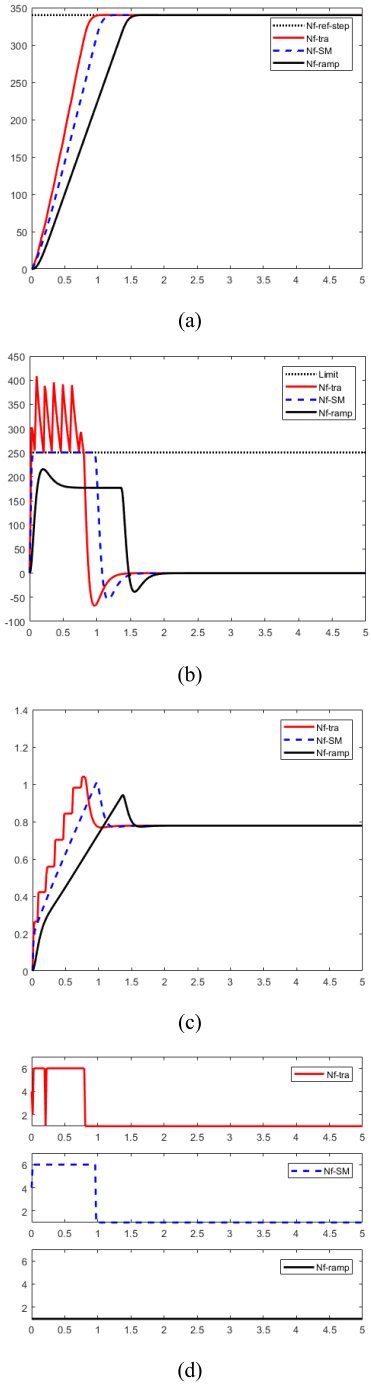

FIGURE 5. The results of the simulation with the variable $\dot{N}_f$. Graph (a) indicates the response of fan speed. Graph (b) indicates the upper output $\dot{N}_f$. Graph (c) indicates the fuel flow input. Graph (d) indicates the switching history. In these graphs, the line (in black) refers to the situation that limits $\dot{N}_f$ with reference ramp, the line (in red) refers to the situation that limits $\dot{N}_f$ with the traditional way, the dotted line (in blue) refers to the situation that limits $\dot{N}_f$ with SMC limiter, and the dotted line (in black) refers to the limit line.

may lead to the high requirements for fuel supply agencies. While with the new method, $\dot{N}_f$ can strictly not exceed the limit while makes full use of the limits, so that it can have a

better performance. Fuel flow input and the switching history are respectively shown in Fig. 5c and Fig. 5d. The basic trend of Fig. 5c is consistent with Fig. 5a. And in Fig. 5d, a conclusion can be drawn that with the new method, the number of switching is greatly reduced, which can improve the effectiveness of the system.

IV. CONCLUSIONS

In this paper, a new control scheme, which is Min-Max/SMC selector structure with core acceleration limiter, is presented. The new scheme can ensure that the engine does not exceed the limits of the full potential of the engine. The simulate results of JT9D turbofan engine linearized model shows that the acceleration/deceleration limiter designed by the Min-Max/SMC method can ensure the core acceleration within the specified range. And the other outputs' limiters designed by the new method can play a good performance. If the acceleration limiter is applied to control fan speed acceleration, compared to the reference ramp input, it will significantly enhance the response and provide a better performance. In summary, the new scheme proposed by this paper is efficient and has a good application prospect.

ACKNOWLEDGMENT

Thanks to the other members of the team for their support to this research.

REFERENCES

[1] C. Chao, D. Yu, W. Bao, and J. Zhao, "Safe protecting switching control for aeroengines based on multiple Lyapunov functions method," in *Proc. 29th Chin. Control Conf.*, Beijing, China, Jul. 2010, pp. 5953–5957.

[2] X. Du, Y.-Q. Guo, and X.-L. Chen, "Limit management of aircraft engine based on nonlinear model predictive control method," *Hangkong Dongli Xuebao/J. Aerosp. Power*, vol. 30, no. 7, pp. 1766–1771, 2015, doi: 10.13224/j.cnki.jasp.2015.07.031.

[3] L. C. Jaw and J. D. Mattingly, *Aircraft Engine Controls: Design, System Analysis, and Health Monitoring*. Reston, VA, USA: AIAA, 2009, p. 384.

[4] D. Yu, X. Liu, W. Bao, and Z. Xu, "Multiobjective robust regulating and protecting control for aeroengines," *J. Eng. Gas Turbines Power*, vol. 131, no. 6, pp. 61601–61610, Jul. 2009, doi: 10.1115/1.2903905.

[5] J. T. Csank, R. D. May, J. S. Litt, and T.-H. Guo, "A sensitivity study of commercial aircraft engine response for emergency situations," NASA Glenn Research Center, Cleveland, OH, USA, Tech. Rep. NASA/TM-2011-217004, 2011.

[6] J. Csank, R. May, J. Litt, and T. H. Guo, "Control design for a generic commercial aircraft engine," in *Proc. 46th AIAA/ASME/SAE/ASEE Joint Propuls. Conf. Exhibit*, Nashville, TN, USA, Jul. 2010, pp. 25–28.

[7] K. J. Åström and T. Hägglund, *PID Controllers: Theory, Design and Tuning*. Pittsburgh, PA, USA: ISA, 1995.

[8] H. A. S. Iii and B. Harold, "Control of jet engines," *Control Eng. Pract.*, vol. 7, no. 9, pp. 1043–1059, Sep. 1999, doi: 10.1016/S0967-0661(99)00078-7.

[9] M. Maggiore, R. Ordóñez, K. M. Passino, and S. Adibhatla, "Estimator design in jet engine applications," *Eng. Appl. Artif. Intell.*, vol. 16, nos. 7–8, pp. 579–593, 2003, doi: 10.1016/j.engappai.2003.10.003.

[10] R. May, J. Csank, T. Lavelle, J. Litt, and T.-H. Guo, "A high-fidelity simulation of a generic commercial aircraft engine and controller," in *Proc. 46th AIAA/ASME/SAE/ASEE Joint Propuls. Conf. Exhibit*, Nashville, TN, USA, Jul. 2010, pp. 25–28.

[11] R. Hanz and S. L. Jonathan, "A novel controller for gas turbine engines with aggressive limit management," in *Proc. 47th AIAA/ASME/SAE/ASEE Joint Propuls. Conf. Exhibit*, San Diego, CA, USA, Aug. 2011, pp. 1–17.

[12] D. M. Ryan and G. Sanjay, "Reducing conservatism in aircraft engine response using conditionally active min-max limit regulators," in*Proc. ASME Turbo Expo, Turbine Tech. Conf. Expo.*, Copenhagen, Denmark, Jun. 2012, pp. 959–968.

[13] R. D. May and S. Garg, "Reducing conservatism in aircraft engine response using conditionally active min-max limit regulators," in *Proc. ASME Turbo Expo, Turbine Tech. Conf. Expo.*, Copenhagen, Denmark, Jun. 2012, pp. 959–968.

[14] Y. Wang, Q. Li, X. Huang, and Y. Zhao, "Controller design for limit protection of aero-engine based on ADRC," *J. Beijing, Univ. Aeronaut. Astronaut.*, vol. 38, no. 9, pp. 1154–1157, 2012, doi: 10.13700/j.bh.1001-5965.2012.09.009.

[15] A. Imani and M. Montazeri-Gh, "Improvement of Min–Max limit protection in aircraft engine control: An LMI approach," *Aerosp. Sci. Technol.*, vol. 68, pp. 214–222, Sep. 2017, doi: 10.1016/j.ast.2017.05.017.

[16] V. K. Ilya, C. J. Link, M. Walt, and H. Van Tran, "Robust control and limit protection in aircraft gas turbine engines," in *Proc. IEEE Int. Conf. Control Appl. (CCA)*, Dubrovnlk, Croatia, Oct. 2012, pp. 812–819.

[17] H. Richter, "A multi-regulator sliding mode control strategy for output-constrained systems," *Automatica*, vol. 47, no. 10, pp. 2251–2259, 2011, doi: 10.1016/j.automatica.2011.08.003.

[18] H. Richter, *Advanced Control of Turbofan Engines*. New York, NY, USA: Springer, 2012.

[19] H. Richter, "Multiple sliding modes with override logic: Limit management in aircraft engine controls," *J. Guid. Control Dyn.*, vol. 35, no. 4, pp. 1132–1142, 2012, doi: 10.2514/1.55922.

[20] A. Imani and M. Montazeri-Gh, "A Min-Max selector controller for turbofan engines with improvement of limit management and low computational burden," *Trans. Inst. Meas. Control*, 2018, pp. 1–9, doi: 10.1177/0142331217752043.

[21] L. Tenghui, S. Xie, and J. Peng, "A design of sliding mode controller for aero-engine based on fuzzy PID approaching law," *J. Air Force Eng. Univ.*, vol. 19, no. 2, pp. 15–20, 2018, doi: 10.3969/j.issn.1009-3516.2018.02.003.

[22] T. Guo, P. Chen, and L. Jaw, "Intelligent life-extending controls for aircraft engines," in *Proc. AIAA 1st Intell. Syst. Tech. Conf.*, Chicago, IL, USA, Sep. 2004, pp. 1–10.

[23] C. L. P. Chen, J. Kim, and T. H. Guo, "Monte Carlo simulation for system damage prediction: An example from thermo-mechanical fatigue (TMF) damage for a turbine engine," in *Proc. IEEE/SMC Int. Conf. Syst. Syst. Eng.*, Los Angeles, CA, USA, Apr. 2006, p. 5.

[24] M. Zhuoguang, X. Shousheng, and Z. Bo, "Adaptive global fast non-singular Terminal sliding mode control for aero-engine," *J. Aerosp. Power*, vol. 28, no. 11, pp. 2634–2640, 2013, doi: 10.13224/j.cnki.jasp.2013.11.031.

[25] H. Ye, M. Chen, and Q. Wu, "Envelope protection control for maneuver flight based on multi-regulator sliding mode control switch approach," *Acta Aeronaut. Astronaut. Sinica*, vol. 35, no. 12, pp. 3358–3370, Dec. 2014, doi: 10.7527/S1000-6893.2014.0067.

[26] S. Zeghlache, K. Kara, and D. Saigaa, "Fault tolerant control based on interval type-2 fuzzy sliding mode controller for coaxial trirotor aircraft," *Isa Trans.*, vol. 59, pp. 215–231, Nov. 2015, doi: 10.1016/j.isatra.2015.09.006.

[27] B. Ganji, A. Z. Kouzani, S. Y. Khoo, and M. Shams-Zahraei, "Adaptive cruise control of a HEV using sliding mode control," *Expert Syst. Appl.*, vol. 41, no. 2, pp. 607–615, 2014, doi: 10.1016/j.eswa.2013.07.085.

[28] L. Jingkun, *Sliding Mode Control Design and MATLAB Simulation the Design Method of Advanced Control System*, 3rd ed. Beijing, China: Tsinghua Univ. Press, 2015.

BING YU received the B.S. degree in automation and the Ph.D. degree in navigation guidance and control from Southeast University, China, in 2002 and 2009, respectively.

His current research interests include the control and testing of the aircraft engine.

HONGWEI KE received the B.S. degree in flight vehicle propulsion engineering from the Nanjing University of Aeronautics and Astronautics, China, in 2017, where he is currently pursuing the master's degree in aerospace propulsion theory and engineering.

WENJUN SHU received the B.S. degree in flight vehicle propulsion engineering from the Nanjing University of Aeronautics and Astronautics, China, in 2016, where he is currently pursuing the master's degree in power machinery and engineering.

TIANHONG ZHANG received the Ph.D. degree from the Nanjing University of Aeronautics and Astronautics in 2001. He is currently a Professor and a Ph.D. Supervisor with the Nanjing University of Aeronautics and Astronautics. His current research interests include aero-engine control, test, and measurement.